Dalton Transactions

Accepted Manuscript

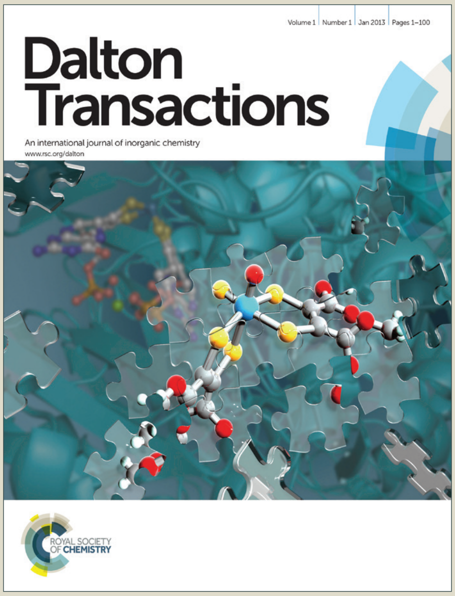

www.rsc.org/dalton

Journal Name

ARTICLE

Received 00th January 20xx,
Accepted 00th January 20xx

DOI: 10.1039/x0xx00000x

www.rsc.org/

Tuning of excitation wavelength in Eu^{3+}-aminophenyl based polyfluorinated β-diketonate complexes: Red-emitting Eu^{3+}-complex encapsulated in silica/polymer hybrid material excited by blue light†

T. V. Usha Gangan[a,b] and M. L. P. Reddy[a,b]*

We describe herein the synthesis, characterization and photophysical properties of a series of europium complexes based on three aminophenyl based polyfluorinated β-diketonates, namely, 1-(4-aminophenyl)-4,4,5,5,5-pentafluoro-3-hydroxypent-2-en-1-one, 1-(4-(dimethylamino)phenyl)-4,4,5,5,5-pentafluoro-3-hydroxypent-2-en-1-one and 1-(4-(diphenylamino)phenyl)-4,4,5,5,5-pentafluoro-3-hydroxypent-2-en-1-one and an ancillary ligand, 4,5-bis(diphenylphosphino)-9,9-dimethylxanthene oxide. The results demonstrated that the triphenylamine based polyfluorinated Eu^{3+}-β-diketonate complexes dramatically red-shifted the excitation maximum to visible region ($\lambda_{ex, max}$ = 400 nm) with impressive quantum yield (40 %) as compared to the simple Eu^{3+}-aminophenyl-β-diketonate complexes ($\lambda_{ex, max}$ = 370 nm). This can be explained on the basis of conjugation between nitrogen lone pair electrons and the phenyl π-electrons in the β-diketonate ligand system. On the other hand, the electron-donating dimethylamino group (Hammett constant: σ_p = -0.83) containing Eu^{3+}-β-diketonate complexes moderately shifted the excitation maximum in the UV region from 370 to 380 nm as compared to unsubstituted aminophenyl (Hammett constant: σ_p = -0.66) Eu^{3+} complexes. The displacement of water molecules in aminophenyl based Eu^{3+}-β-diketonate binary complexes by a rigid phosphine oxide ligand richly enhances the photoluminescence quantum yields as well as the excited state lifetime values of the corresponding ternary complexes. As an integral part of this work, hybrid materials have been developed through sol-gel route by encapsulating a ternary Eu^{3+} compound in a silica/polymer hybrid for high performamnce luminescence applications. In addition, a bright red-emitting diode was fabricated by coating the designed hybrid material onto a 400 nm emitting InGaN chip and examined the photoluminescence. Notably, the current study clearly highlights that the developed triphenylamine based Eu^{3+}-β-diketonate complex is an interesting red-emitting material excited by blue light and therefore may find potential application in the fields of biological and material sciences.

Introduction

The unique photoluminescence properties of Eu^{3+} complexes have aroused tremendous interest for decades owing to their outstanding potential applications in medical diagnostics and organic light emitting diodes.[1-4] The shielding of the f orbitals by the $5s^2$ and $5p^6$ closed shells results in narrow line-like emissions of optically pure colors with long radiative lifetimes. However, the f-f transition that result in light emission from the lanthanide ions are both spin-and parity-forbidden which, in turn, mandates the use of antenna molecules for the indirect excitation of the metal center. This indirect excitation, also known as antenna effect, takes advantage of the coordinated ligands in the sense that energy transfer from the ligand-centered excited states to the metal center results in lanthanide ion luminescence.[4] The β-diketonate ligand class is emerging as one of the important antenna molecules in terms of high harvest emissions because of the effectiveness of the energy transfer from this ligand to the Ln^{3+} ion.[5]

Unfortunately, the excitation window appears to be limited to the near-UV region in many of the Eu^{3+}-β-diketonate complexes due to the energy constraints posed by the photophysics of sensitized Eu^{3+} luminescence, as well documented by Reinhoudt and coworkers.[6] Therefore, one of the challenges in this field is to develop luminescent Eu^{3+} complexes that can be excited by visible light and this field has become more important because of the increasing demand for less harmful reagents in life sciences and also low voltage driven pure red emitters in optoelectronic applications. Indeed, some of the recent literature reports demonstrated

---

[a] *AcSIR-Academy of Scientific & Innovative Reasearch, CSIR-NIIST Campus, Thiruvananthapuram, India*
[b] *Materials Science and Technology Division, National Institute for Interdisciplinary Science and Technology (NIIST), Council of Scientific and Industrial Research (CSIR), Thiruvananthapuram-695 019, India, E-mail: mlpreddy55@gmail.com*

†Electronic Supplementary Information (ESI) available: ^1H NMR, ^{13}C NMR spectra of the ligands, thermogravimetric curves for complexes and gels, lifetime decay profiles, photochemical stability, FT-IR spectra of the hybrid materials, UV-visible absorption spectra of the hybrid materials in solid state and XRD patterns of the hybrid materials.

that the excitation window can be shifted to visible region in Eu^{3+}-β-diketonate complexes by appropriate molecular engineering of the ligand systems with suitably expanded π-conjugation in the complex molecules.[7-9] However, some of the Eu^{3+}-β-diketonate complexes reported exhibit poor quantum yields.[7,8*a*,*b*]

Triphenylamine derivatives are widely used as hole-transporting materials in Organic Light Emitting Diodes (OLEDs) due to their high charge mobility, light-harvesting unit and high thermal stability.[10] It is well documented that the replacement of C–H bonds in a β-diketonate ligand with lower-energy C–F oscillators is able to lower the vibration energy of the ligand, which decreases the energy loss caused by ligand vibration and enhances the emission intensity of the lanthanide ion. Further, due to the heavy-atom effect, which facilitates intersystem crossing, the lanthanide-centered luminescent properties are enhanced.[11] Based on the above considerations, we conceive of a strategy that simultaneously incorporates highly conjugated triphenylamine and polyfluorinated alkyl groups into the β-diketonate ligand, expecting to obtain the resultant ligands possessing high luminescence efficiency and photochemical stability under visible light excitation upon coordination with trivalent lanthanides. Thus, a series of novel aminophenyl based β-diketonate ligands (Scheme 1), namely, 1-(4-aminophenyl)-4,4,5,5,5-pentafluoro-3-hydroxypent-2-en-1-one (HAPFP), 1-(4-(dimethylamino)phenyl)-4,4,5,5,5-pentafluoro-3-hydroxypent-2-en-1-one (HDMAPFP) and 1-(4-(diphenylamino)phenyl)-4,4,5,5,5-pentafluoro-3-hydroxypent-2-en-1-one (HDPAPFP) have been synthesized and utilized for the construction of Eu^{3+}-β-diketonate coordination compounds in the presence and absence of an ancillary ligand, 4,5-bis(diphenylphosphino)-9,9-dimethylxanthene oxide (DDXPO) with a view to shift the excitation window to the visible region. Herein, we demonstrate that these ligands are easily accessible, readily coordinate to europium, and efficiently sensitize its luminescence when excited under visible light. The origin of “amino conjugation effect” on the emission as well as other excited state properties in these complexes has also been elucidated and discussed.

Due to their poor thermal resistivity, moisture sensitivity and feeble mechanical strength, the lanthanide complexes are difficult to directly utilize as luminescence sources in many optoelectronic applications. These inherent problems can be solved by encapsulating the lanthanide luminescent complexes in suitable solid matrixes including polymers,[2*a*,4*d*,8*c*,12] sol-gel silica,[2*a*,3*c*,4*d*,13] mesoporous materials[2*a*,4*d*,5*g*,8*c*,14] and even carbon nanotubes.[8*d*,15] The potential utility of these materials depend on exploiting the synergy between the excellent luminescence features of lanthanides and the intrinsic characteristics of sol-gel derived hybrid materials. These materials may find promising applications such as light emitting devices, active wave guides and biomedical actuators and sensors. In order to enhance the luminescent properties and improve the stability of the lanthanide complexes, herein, a novel ternary Eu^{3+} luminescent complex has been embedded into silica/polymer hybrid material, characterized and examined the photoluminescence properties. Additionally, a bright red emitting diode was fabricated by coating the luminescent hybrid material onto a 400 nm emitting InGaN chip and investigated the photoluminescence.

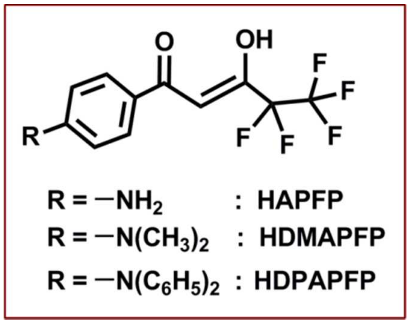

Scheme 1 Structures of the β-diketonate ligands.

Experimental Section

Materials and instrumentation

The following chemicals were acquired commercially and used without further purification: Europium(III) nitrate hexahydrate, 99.9% (Alfa-Aesar); gadolinium(III) nitrate hexahydrate, 99.9% (Sigma-Aldrich); triphenylamine, 98% (Sigma-Aldrich); 4-aminoacetophenone, 99% (Alfa-Aesar); sodium hydride 60% dispersion in mineral oil (Sigma-Aldrich); ethyl pentafluoropropionate, 98% (Sigma-Aldrich); 4,5-bis(diphenylphosphino)-9,9-dimethylxanthene, 97% (Sigma-Aldrich); iodomethane, 98% (Alfa-Aesar); Tetraethyl orthosilicate (TEOS), 98% (Sigma-Aldrich). All the other chemicals used were of analytical reagent grade without further purification.

Elemental analyses were performed with an Elementar - vario MICRO cube elemental analyzer. A Perkin-Elmer Spectrum two FT-IR spectrometer using KBr was used to obtain the IR spectral data and a Bruker 500 MHz NMR spectrometer was used to record the ^{1}H NMR (500 MHz), ^{13}C NMR (125.7 MHz) and ^{31}P NMR (202.44 MHz) spectra of the new compounds in chloroform-d solution. The chemical shifts are reported in parts per million relative to tetramethylsilane, $SiMe_4$ for ^{1}H NMR and ^{13}C NMR spectra and with respect to 85% phosphoric acid for ^{31}P NMR spectra. Electro spray ionization (ESI) mass spectra were recorded on a Thermo Scientific Exactive Benchtop LC/MS Orbitrap Mass Spectrometer. Matrix assisted laser desorption ionization time-of-flight (MALDI-TOF) mass spectra were recorded on KRATOS analytical spectrometer (Shimadzu Inc.) and the thermogravimetric analyses were performed on a TG/DTA-6200 (SII Nano Technology Inc., Japan). Scanning electron microscopy (SEM) of EuC-PMMA-Gel and EuC-Gel were performed on a ZEISS EVO-18 Cryo-SEM instrument. X-ray powder patterns (XRD) were recorded in the 2θ range of 10-70° using Cu-K$_{\alpha}$ radiation (Philips X'pert Pro). The molar absorption coefficient (ε) of the ligands were measured in THF solution on a UV-vis spectrophotometer (Shimadzu, UV-2450). The photoluminescence (PL) spectra were recorded on a Spex-Fluorolog FL22 spectrofluorimeter equipped with a double grating 0.22 m Spex 1680 monochromator and a 450W Xe lamp as the excitation source operating in the front face mode. The lifetime measurements were carried out at room temperature using a Spex 1040D phosphorimeter. The overall quantum yield (Φ_{overall}) was measured using an integrating sphere in a SPEX Fluorolog spectrofluorimeter.

The PL quantum yields of thin films (Φ_{overall}) were determined using a calibrated integrating sphere system. A Xe-arc lamp was used to excite the thin film samples that were placed in the sphere. All samples were prepared by drop casting the material placed between two glass cover slips. The quantum yields were determined by comparing the spectral intensities of the lamp and the sample emission as reported in the literature.[16] Using this experimental setup and the integrating sphere system, the solid state fluorescence quantum yield of a thin film of the standard green OLED material tris-8-hydroxyquinolinolato aluminium (Alq_3) was determined to be 0.40, which is consistent with previously reported values.[17] Several measurements were carried out for each sample, so that the presented value corresponds to the arithmetic mean value. The estimated error for the quantum yields is (± 10%).

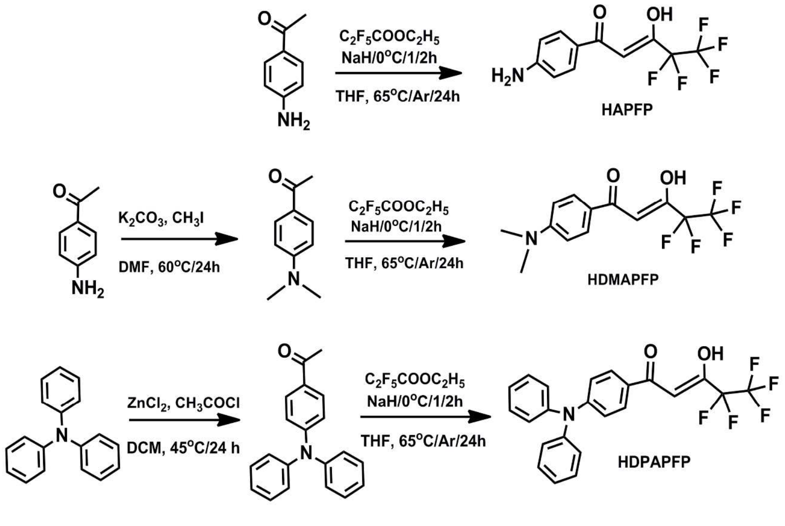

Scheme 2 Synthetic procedure for the ligands.

Synthetic procedures

The ligands 1-(4-aminophenyl)-4,4,5,5,5-pentafluoro-3-hydroxypent-2-en-1-one (HAPFP), 1-(4-(dimethylamino)phenyl)-4,4,5,5,5-pentafluoro-3-hydroxypent-2-en-1-one (HDMAPFP) and 1-(4-(diphenylamino)phenyl)-4,4,5,5,5-pentafluoro-3-hydroxypent-2-en-1-one (HDPAPFP) were synthesized according to the method described in scheme 2.

Synthesis of 1-(4-(dimethylamino)phenyl)ethanone. To a DMF solution of 4-aminoacetophenone (7.40 mmol) iodomethane (17 mmol) and K_2CO_3 (17 mmol) were added. The resultant mixture was stirred at 60 °C for 1 day, cooled at room temperature and quenched with a mixture of ice and water. The product was filtered and washed with water to afford the compound as a white solid. Yield: 82%. ^{1}H NMR ($CDCl_3$, 500 MHz) δ (ppm): 7.87 (d, 2H, J = 8.5 Hz), 6.65 (d, 2H, J = 8.5 Hz), 3.06 (s, 6H), 2.51 (s, 3H). ^{13}C NMR ($CDCl_3$, 125.7 MHz) δ (ppm): 196.47, 153.17, 130.53, 125.33, 129.60, 110.59, 40.02, 25.98. m/z = 164 $(M+H)^+$.

Synthesis of 1-(4-(diphenylamino)phenyl)ethanone. Acetyl chloride (4.08 mmol) taken in dichloromethane solution was added dropwise to a slurry of zinc chloride (4.08 mmol) suspended in a solution of triphenylamine (4.08 mmol). After the addition was completed, the mixture was heated under reflux for 24 h. The reaction mixture was then poured into cold, dilute hydrochloric acid. The organic layer was separated, washed with water until the wash water was neutral, and then dried over anhydrous sodium sulphate. The resulting residue was purified by column chromatography using ethyl acetate/hexane (10:90), thereby affording the desired product as a yellow solid. Yield: 60%. ^{1}H NMR ($CDCl_3$, 500 MHz) δ (ppm): 7.79 (d, 2H, J = 10 Hz), 7.30 (m, 4H), 7.14 (m, 6H), 6.98 (d, 2H, J = 9 Hz), 2.53 (s, 3H). ^{13}C NMR ($CDCl_3$, 125.7 MHz) δ (ppm): 196.48, 152.17, 146.51, 129.88, 129.60, 125.96, 124.63, 119.68, 26.23. m/z = 288 $(M+H)^+$.

Synthesis of the ligands. A modified method of typical Claisen condensation procedure is used for the synthesis of β-diketonate ligands. The corresponding ketone (1.0 mmol) and ethyl pentafluoropropionate (1.0 mmol) were added to 20 mL of dry tetrahydrofuran (THF) and stirred for 10 min at 0 °C in an ice bath. To this reaction mixture, sodium hydride (60%) was added in an inert atmosphere and stirred for 30 min followed by further stirring at 65 °C for 24 h. To the resulting solution, 2 M HCl (25 mL) was added, and extracted thrice with dichloromethane (3 × 25 mL). The organic layer was separated and dried over Na_2SO_4, and the solvent was evaporated. The crude product thus obtained was then purified by column chromatography on silica gel with mixture of ethyl acetate and hexane (5:95 for HAPFP, 2:98 for HDMAPFP and HDPAPFP) as the eluent to get the product.

1-(4-aminophenyl)-4,4,5,5,5-pentafluoro-3-hydroxypent-2-en-1-one (HAPFP). Yield: 60%. Elemental analysis (%): calculated for $C_{11}H_8F_5NO_2$ (281.18): C 46.99, H 2.87, N 4.98; Found: C 46.74, H 2.84, N 4.76. ^{1}H NMR ($CDCl_3$, 500 MHz) δ (ppm): 15.28 (broad, enol–OH), 8.17 (s, 2H, NH_2), 8.04 (d, 2H, J = 9 Hz), 7.79 (d, 2H, J = 8.5 Hz), 6.64 (S, 1H). ^{13}C NMR (125.7 MHz, $CDCl_3$) δ (ppm): 196.68, 183.78, 156.39, 139.88, 132.16 127.21, 117.21, 112.14, 96.82, 77.26-76.75 ($CDCl_3$). IR (KBr) ν_{max} (cm^{-1}): 3346 (N-H), 1703, 1534, 1333, 1209, 1037, 794. *m/z* = 281 (M)$^+$.

1-(4-(dimethylamino)phenyl)-4,4,5,5,5-pentafluoro-3-hydroxypent-2-en-1-one (HDMAPFP). Yield: 65%. Elemental analysis (%): calculated for $C_{13}H_{12}F_5NO_2$ (309.23): C 50.49, H 3.91, N 4.53; Found: C 50.64, H 4.06, N 4.58. ^{1}H NMR ($CDCl_3$, 500 MHz) δ (ppm): 15.97 (broad, enol–OH), 7.86 (d, 2H, J = 9.5 Hz), 6.68 (d, 2H, J = 10 Hz), 6.48 (s, 1H), 3.11 (S, 6H). ^{13}C NMR ($CDCl_3$, 125.7 MHz) δ (ppm): 185.68, 175.78, 154.39, 133.88, 130.20, 127.21, 119.21, 111.14, 91.82, 40.02, 77.28-76.78 ($CDCl_3$). IR (KBr) ν_{max} (cm^{-1}): 2925, 1586, 1377, 1329, 1229, 1011, 741. *m/z* = 310.08 (M+H)$^+$.

1-(4-(diphenylamino)phenyl)-4,4,5,5,5-pentafluoro-3-hydroxypent-2-en-1-one (HDPAPFP). Yield: 85%. Elemental analysis (%): calculated for $C_{23}H_{16}F_5NO_2$ (433.37): C 63.74, H 3.72, N 3.23; Found: C 63.90, H 3.84, N 3.35. ^{1}H NMR ($CDCl_3$, 500 MHz) δ (ppm): 15.71 (broad, enol–OH), 7.78 (d, 2H, J = 9 Hz), 7.35 (m, 4H), 7.20 (m, 6H), 6.98 (d, 2H, J = 8.5 Hz), 6.50 (s, 1H) (Fig. S1). ^{13}C NMR ($CDCl_3$, 125.7 MHz) δ (ppm): 189.63, 185.74, 153.39, 145.83, 130.10, 129.88, 129.79, 129.48, 126.39, 125.42, 123.80, 119.06, 92.45, 77.27-76.76 ($CDCl_3$). IR (KBr) ν_{max} (cm^{-1}): 3059, 1609, 1585, 1490, 1331, 1265, 1016, 697. *m/z* = 434.22 (M+H)$^+$.

4,5-Bis(diphenylphosphino)-9,9-dimethylxanthene oxide (DDXPO). The corresponding phosphine (5.0 mmol) was dissolved in 10 mL of 1,4-dioxane solution, to which 1.0 mL of 30% H_2O_2 (10.5 mmol) was added drop wise with vigorous stirring. The resultant mixture was then stirred for 2 h and then 10 mL of water was added to the reaction mixture to arrest the reaction. The mixture was extracted with 3 × 30 mL of dichloromethane. The oily phase was then washed with 2 × 30 mL of water to remove 1,4-dioxane. The dichloromethane layer was dried with Na_2SO_4. The solvent was removed in *vacuo*. The product was recrystallized from dichloromethane. Yield: 95%. Elemental analysis (%): calculated for $C_{39}H_{32}O_3P_2$ (610.18): C 76.71, H 5.28; Found: C 76.52, H 5.40. ^{1}H NMR ($CDCl_3$, 500 MHz) δ (ppm): 7.61 (d, 2 H, J = 5 Hz), 7.41 (q, 12 H, J = 20 Hz), 7.30 (q, 8 H, J = 20 Hz), 6.99 (m, 2 H), 6.80–6.76 (q, 2 H, J = 20 Hz), 1.70 (s, 6 H). ^{31}P NMR ($CDCl_3$, 202.44 MHz) δ (ppm): 30.97. IR (KBr) ν_{max} (cm^{-1}): 1727, 1670, 1436, 1401, 1229, 1190, 1114, 875, 785, 746, 719, 694. *m/z* = 611.31 (M+H)$^+$.

Synthesis of binary complexes. To a solution of β-diketonate ligand (3.0 mmol) in ethanol, NaOH (3.0 mmol) in water was added and stirred for 5 min. To this mixture, $Ln(NO_3)_3{\cdot}6(H_2O)$ (where Ln = Eu^{3+}, Gd^{3+}) (1.0 mmol) in 2 mL water was added drop wise and stirred for 12 h at room temperature. The resultant precipitate formed was filtered off, washed with water and dried. The products were purified by recrystallization from chloroform solution and used for further analysis and photophysical studies. Efforts to grow single crystals of complexes were not fruitful. The synthesis method is described in Scheme 3.

$Eu(APFP)_3(H_2O)_2$ (1). Elemental analysis (%): calculated for $C_{33}H_{25}F_{15}N_3O_8Eu$ (1029.06): C 38.54, H 2.45, N 4.09; Found: C 38.35, H 2.53, N 3.93. IR (KBr) ν_{max} (cm^{-1}): 3435, 3320, 1712, 1523, 1328, 1216, 1039, 695. *m/z* = 1016.28 $[Eu(APFP)_3{+}Na{+}1]^+$.

$Eu(DMAPFP)_3(H_2O)_2$ (**2**). Elemental analysis (%): calculated for $C_{39}H_{37}F_{15}N_3O_8Eu$ (1113.16): C 42.10, H 3.35, N 3.78; Found: C 42.25, H 3.33, N 3.87. IR (KBr) ν_{max} (cm^{-1}): 3443, 2927, 1594, 1370, 1323, 1281, 1014, 671. *m/z* = 1094.44 $[Eu(DMAPFP)_3(H_2O)]^+$.

$Eu(DPAPFP)_3(H_2O)_2$ (3). Elemental analysis (%): calculated for $C_{69}H_{49}F_{15}N_3O_8Eu$ (1485.25): C 55.80, H 3.33, N 2.83; Found: C 56.01, H 3.45, N 2.91. IR (KBr) ν_{max} (cm^{-1}): 3437, 3049, 1614, 1583, 1492, 1327, 1275, 1013, 678. *m/z* = 1447.33 $[Eu(DPAPFP)_3{-}H]^+$.

$Gd(APFP)_3(H_2O)_2$(7). Elemental analysis (%): calculated for $C_{33}H_{25}F_{15}N_3O_8Gd$ (1034.06): C 38.34, H 2.44. N 4.06; Found: C 38.20, H 2.18, N 3.91. IR (KBr) ν_{max} (cm^{-1}): 3435, 3321, 1711, 1523, 1328, 1216, 1039, 695. *m/z* = 1016.48 $[Gd(APFP)_3(H_2O)]^+$.

$Gd(DMAPFP)_3(H_2O)_2$(8). Elemental analysis (%): calculated for $C_{39}H_{37}F_{15}N_3O_8Gd$ (1118.16): C 41.90, H 3.35. N 3.76; Found: C 42.06, H 3.26, N 3.68. IR (KBr) ν_{max} (cm^{-1}): 3443, 2927, 1595, 1370, 1323, 1281, 1014, 671. *m/z* = 1141.89 $[Gd(DMAPFP)_3(H_2O)_2{+}Na]^+$.

$Gd(DPAPFP)_3(H_2O)_2$ (9). Elemental analysis (%): calculated for $C_{71}H_{55}F_{15}N_3O_8Gd$ (1454.23): C 55.61, H 3.31. N 2.82; Found: C 55.78, H 3.43, N 2.98. IR (KBr) ν_{max} (cm^{-1}): 3433, 3054, 1615, 1584, 1492, 1327, 1276, 1013, 698. *m/z* = 1022.30 $[Gd(DPAPFP)_2]^{+\cdot}$

Synthesis of Eu^{3+} complexes 4-6. Ternary Eu^{3+} complexes were prepared by stirring equimolar solutions of corresponding binary complexes and DDXPO in $CHCl_3$ solution for 12 h at 70 °C. The products were isolated by solvent evaporation and purified by recrystallization from a chloroform mixture. The synthesis procedure is illustrated in scheme 4.

$Eu(APFP)_3$(DDXPO) (4). Elemental analysis (%): calculated for $C_{72}H_{53}O_9F_{15}N_3P_2Eu$ (1603.22): C 53.94, H 3.33, N 2.62; Found: C 54.06, H 3.44, N 2.65. IR (KBr) ν_{max} (cm^{-1}): 3060, 1713, 1527, 1333, 1217, 1179, 1019, 696. *m/z* = 1345.83 $[Eu(APFP)_2(DDXPO){+}Na]^+$. ^{31}P NMR ($CDCl_3$, 202.44 MHz) δ (ppm): -77.55.

$Eu(DMAPFP)_3$(DDXPO) (5). Elemental analysis (%): calculated for $C_{78}H_{65}O_9F_{15}N_3P_2Eu$ (1687.32): C 54.52, H 3.88, N 2.49; Found: C 54.39, H 4.01, N 2.45. IR (KBr) ν_{max} (cm^{-1}): 3061, 1596, 1506, 1403, 1330, 1274, 1179, 1014, 676. *m/z* = 1402.20 $[Eu(DMAPFP)_2(DDXPO){+}Na{+}1]^+$. ^{31}P NMR ($CDCl_3$, 202.44 MHz) δ (ppm): -82.80.

$Eu(DPAPFP)_3$(DDXPO) (6). Elemental analysis (%): calculated for $C_{108}H_{77}O_9F_{15}N_3P_2Eu$ (2059.67): C 62.98, H 3.77, N 2.04;

Found: C 63.02, H 3.92, N 2.11. IR (KBr) ν_{max} (cm^{-1}): 3061, 1622, 1588, 1524, 1492, 1327, 1274, 1178, 1013, 696. *m/z* = 1628.93 [Eu(DPAPFP)$_2$(DDXPO)]$^+$. ^{31}P NMR (CDCl$_3$, 202.44 MHz) δ (ppm): -86.87.

Synthesis of Eu(DPAPFP)$_3$(DDXPO)-Gel [EuC-Gel]. Tetraethyl orthosilicate (TEOS) was first mixed with ethanol, and then HCl-acidified water (pH = 2) was added to the above mixture under magnetic stirring to initiate the hydrolysis and condensation reaction. The molar ratio of TEOS/ethanol/H_2O was maintained at 1:4:4. A transparent sol was obtained. After stirring for 3 h, N,N-dimethylformamide (DMF) solution containing an appropriate amount of the ternary complex Eu(DPAPFP)$_3$(DDXPO) (the mass ratio of Eu^{3+} complex (**6**)/SiO$_2$ was 3:10) was added to the sol. The mixture was stirred at room temperature for 4 h. The gel was allowed to stand for 5 days and then dried at 45 °C. The gel was collected as monolithic bulks and ground into powdered material for the photophysical studies.

Synthesis of Polymer-Eu(DPAPFP)$_3$(DDXPO)-Gel (EuC-PMMA-Gel). Similar to the EuC-Gel preparation, TEOS was first mixed with ethanol. Then HCl-acidified water (pH = 2) was added to start the hydrolysis and condensation reaction. The molar ratio of TEOS/ethanol/H_2O was 1:4:4. After stirring for 3 h, DMF solution containing the complex Eu(DPAPFP)$_3$(DDXPO) and polymer (PMMA) were added to the sol. The mass ratio of Eu^{3+} complex/PMMA/SiO$_2$ was 3:4:10. The mixture was stirred for 4h at room temperature to make sure uniform mixing and complete hydrolysis, and then placed in a sealed container, which was kept at 45 °C until the precursor solution was converted into a monolithic gel and ground into powdered material for the photophysical studies.

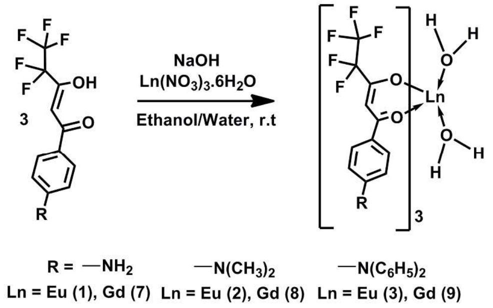

Scheme 3 Synthesis of the Ln^{3+} (Ln = Eu, Gd) binary complexes.

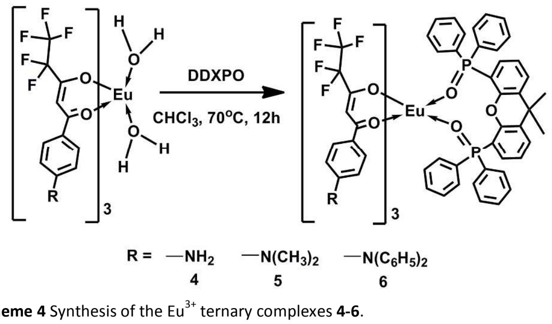

Scheme 4 Synthesis of the Eu^{3+} ternary complexes **4**-**6**.

Results and discussion

Synthesis and characterization of lanthanide complexes

Scheme 2 summarizes the protocols used for the synthesis of various β-diketonates that are used in the present study. The β-diketonates (HAPFP, HDMAPFP and HDPAPFP) were obtained as yellow solids in 60-85% yields by Claisen condensation of the corresponding ketones with ethyl pentafluoropropionate in the presence of a strong base NaH. Detailed characterisation of the synthesized ligands was performed by ^{1}H NMR, ^{13}C NMR (Fig. S1 to S6 in the ESI†), ^{31}P NMR, FT-IR and mass spectroscopic (ESI-MS) methods, as well as by elemental analysis. ^{1}H NMR analysis shows that the β-diketonate compounds mainly exist as enol form in chloroform solutions. The chelating ligand 4,5-bis(diphenylphosphino)-9,9-dimethylxanthene oxide (DDXPO) was synthesized according to the previous literature report.[5e,f] The synthesis procedures for the Ln^{3+} (Eu^{3+} and Gd^{3+}) complexes are depicted in Schemes 3 and 4, respectively. The lanthanide complexes were characterized by FT-IR, MALDI-TOF and elemental analysis. The elemental analysis and MALDI-TOF studies of Ln^{3+} complexes (**1**-**9**) revealed that the central Ln^{3+} ion is coordinated to three β-diketonate ligands. In the case of ternary complexes (**4**-**6**), one molecule of the bidentate phosphine oxide, DDXPO, is also present in the coordination sphere, which is confirmed by FT-IR analysis. Shift in the P=O stretching frequency of DDXPO 1190 cm^{-1} to 1179 cm^{-1} in ternary complexes **4**-**6** confirms the participation of phosphoryl oxygen in the complex formation with the metal ion. This has been further confirmed from the ^{31}P NMR spectra of the complexes **4**-**6** that the P=O resonances are shifted upfield compared to the free ligand, indicating the involvement of phosphoryl oxygen in coordination with the Eu^{3+} ion. The broad absorption band noted in the region 3000 – 3500 cm^{-1} of the FT-IR spectra of the complexes (**1**-**3** and **7**-**9**), points to the existence of water molecules in the coordination sphere. On the other hand, the absence of this broad band in complexes **4**–**6** inferred that the water molecules have been displaced successfully by the chelating phosphine oxide ligand. The carbonyl stretching frequency of the β-diketonate ligands, HAPFP (1703 cm^{-1}), HDMAPFP (1586 cm^{-1}), HDPAPFP (1609 cm^{-1}) is shifted to higher wave numbers in **1**–**9** (1712 cm^{-1} in **1**; 1594 cm^{-1} in **2**; 1614 cm^{-1} in **3**; 1713 cm^{-1} in **4**; 1596 cm^{-1} in **5**; 1622 cm^{-1} in **6**, 1711 cm^{-1} in **7**; 1595 cm^{-1} in **8** and 1615 cm^{-1} in **9**), thus confirming the coordination of the carbonyl oxygen to the Ln^{3+} ions.

The thermal behaviour of the Ln^{3+} complexes were investigated by means of thermogravimetric analysis (TGA) under a nitrogen atmosphere and the results are given in the Fig. S7 in ESI.† It is clear from the thermogravimetric analysis data that complexes **1**-**3** and **7**-**9** undergoes a mass loss of about 3% in the first step (90 to 140 °C), which corresponds to the elimination of the coordinated water molecules. On the other hand, complexes **4**-**6** are more stable than the precursor samples **1**-**3** and do not show decomposition up to 250 °C. The total weight loss occurred in the thermal analysis of all these complexes are much higher than that calculated values for the non-volatile lanthanide(III) oxide, indicating the partial sublimation of these complexes under atmospheric pressure, which is commonly observed in the case of fluorinated β-diketonate complexes.[5f]

Electronic spectra of the aminophenyl based β-diketonate ligands and their corresponding Eu^{3+} complexes (1-6)

The absorption spectra of the free ligands and the corresponding Eu^{3+} complexes (**1**-**6**) have been recorded in THF solution (c = 5 × 10^{-6} M) at 298 K and are depicted in Figs. 1 and 2, respectively. The absorption profiles of the Eu^{3+} complexes in THF solution are found to be similar to that of the ligands, indicating that the singlet excited states of the ligand is not significantly affected by complexation to the Eu^{3+} ion. The main absorption band of all the β-diketonate ligands (singlet-singlet n-π^* enolic transition: 290-380 nm in HAPFP with λ_{max} = 350 nm; 340-470 nm in HDMAPFP with λ_{max} = 420 nm; 340-490 nm in HDPAPFP with λ_{max} = 425 nm), on complexation with Eu^{3+} ion, underwent a hypsochromic shift (~ 10 nm in **1** and **4**; ~ 35-45 nm in **2** and **5**; ~ 38-45 nm in **3** and **6**), while the short wavelength band (π-π^* transition of aromatic moiety of the β-diketonate ligand: 250-305 nm in **1** and **4**; 275-325 nm in **2** and **5**; 275-340 nm in **3** and **6**) remains unaffected. This indicates that the electron density on the diketonate moiety has been perturbed by the imposed negative charge of deprotonation and presence of Lewis acidic metal centre, while the aromatic part retains the same strength.[5f,18] The electronic transitions of the aromatic moiety of the β-diketonate ligand (peak at ca. 250-320 nm) and the chelated phosphine oxide (peak at ca. 250-300 nm) units are overlapped. The presence of the ancillary ligand DDXPO not only enhances the absorption intensity but also satisfies the high coordination number of the central Eu^{3+} ion and thus improves the coordination and thermal stabilities of ternary complexes. The extinction coefficients (Table 1) of the complexes (**1**-**6**) are about three times higher compared to that of the free ligand, in line with the formation of 3:1 (ligand : metal). These features point to the ligand being an adequate light-harvesting chromophore for the sensitization of Eu^{3+} luminescence.[5a-g,8]

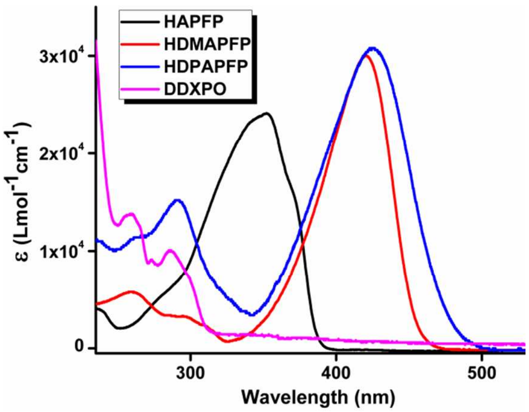

Fig. 1 UV-visible absorption spectra of the ligands HAPFP, HDMAPFP, HDPAPFP and DDXPO in THF (c = 5 × 10^{-6} M).

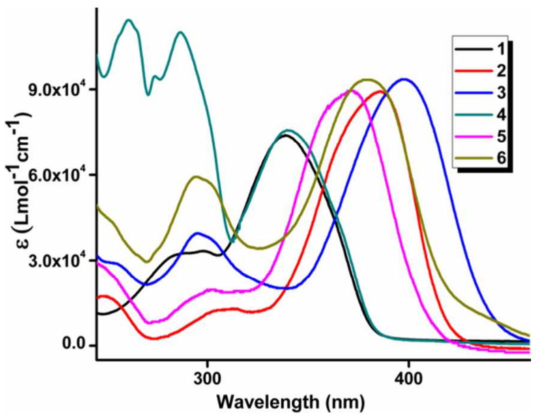

Fig. 2 UV-visible absorption spectra of complexes **1**-**6** in THF (c = 5 × 10^{-6} M).

Table 1 Molar absorption coefficient for the ligands and their corresponding Eu^{3+} complexes

Compounds	λ_{max} (nm)	ε (L mol^{-1} cm^{-1})
HAPFP	350	2.40 × 10^4
HDMAPFP	420	2.96 × 10^4
HDPAPFP	425	3.08 × 10^4
$Eu(APFP)_3(H_2O)_2$ (**1**)	340	7.30 × 10^4
$Eu(DMAPFP)_3(H_2O)_2$ (**2**)	385	8.91 × 10^4
$Eu(DPAPFP)_3(H_2O)_2$ (**3**)	398	9.32 × 10^4
$Eu(APFP)_3(DDXPO)$ (**4**)	340	7.45 × 10^4
$Eu(DMAPFP)_3(DDXPO)$ (**5**)	375	8.90 × 10^4
$Eu(DPAPFP)_3(DDXPO)$ (**6**)	380	9.28 × 10^4

Solid-state photophysical properties of Eu^{3+} complexes 1-6

The solid-state normalized excitation spectra of the Eu^{3+} binary (**1**-**3**) and ternary complexes (**4**-**6**) recorded at 298 K are displayed in Figs. 3 and 4, respectively. The excitation profiles were recorded by monitoring the intense $^5D_0 \rightarrow {}^7F_2$ (612 nm) transition of the Eu^{3+} ion. The excitation spectra of the compounds (**1**-**6**) exhibit a broad band between 250 - 500 nm, which is attributable to the π-π^* transition of the coordinated ligands. The absence of any absorption bands due to the f-f transitions of the Eu^{3+} ion proves that luminescence sensitization *via* excitation of the ligand is effective. The replacement of hydrogen ions in aminophenyl based β-diketonate ligand with a highly conjugated phenyl moieties significantly influences the π-conjugation in the complex molecules of the Eu^{3+} (**3** and **6**) and shifts the excitation window to the visible region ($\lambda_{ex,max}$ = 400 nm), with important applications in biomedical analysis and lighting devices.[1-4] The introduction of *N*-phenyl substituent in aminophenyl based β-diketonate ligand results in considerable bathochromic shifts in the excitation wavelength (~30 nm in **3** and **6**), suggesting the substantial interactions between the *N*-phenyl and aminophenyl β-diketonate moieties. Indeed, it has been suggested for triphenylamine and its derivatives, there is a strong conjugation between the nitrogen lone pair electrons and the phenyl π-electrons, and that the whole molecule is a

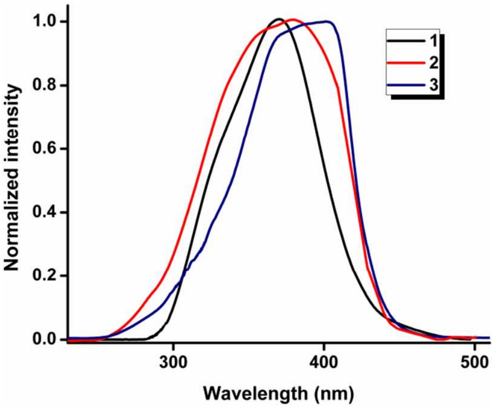

Fig. 3 Normalized excitation spectra of Eu^{3+} binary complexes **1**-**3** in solid state.

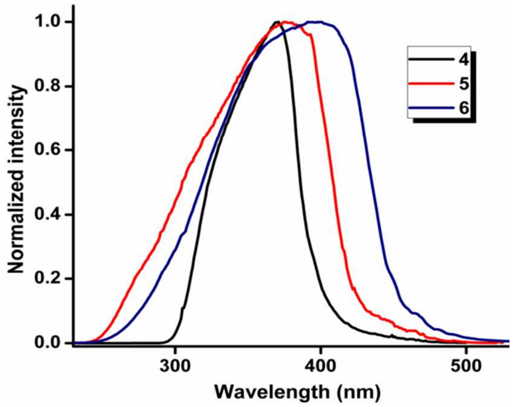

Fig. 4 Normalized excitation spectra of Eu^{3+} ternary complexes **4-6** in solid state.

new chromophore with characteristic absorption and excitation profiles.[10*b*,19] Here the resonance effect plays major role compared to electron donating effect in shifting the excitation maximum. On the other hand, the presence of electron-donating dimethylamino group in Eu^{3+} complexes **2** and **5** moderately red shifted the excitation window in the UV region ($\lambda_{ex,max}$ = 380 nm) as compared to the parent Eu^{3+} complexes **1** and **4** ($\lambda_{ex,max}$ = 370 nm).[18*a*] The donating capacity can be described by Hammett substituent constant, σ_p which represents a situation where the substituent is directly attached with the reaction centre in an electron demanding state. The Hammett constants, σ_p for $N(CH_3)_2$ is -0.83 and for NH_2 σ_p = -0.66, clearly explains the observed behaviour.[20]

The ambient-temperature emission spectra of Eu^{3+} complexes **1**-**6** excited at their corresponding excitation maxima (λ_{ex} = 370 nm for complexes **1** and **4**; λ_{ex} = 380 nm for complexes **2** and **5**; λ_{ex} = 400 nm for complexes **3** and **6**) exhibit characteristic narrow emission bands arising from the intra-configurational $^5D_0 \rightarrow {}^7F_J$ (J = 0-4) transitions of the Eu^{3+} ion (Fig. 5).

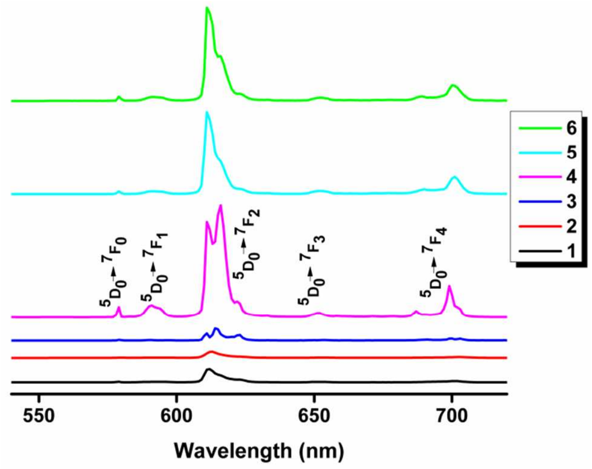

Fig. 5 298 K emission spectra of Eu^{3+} complexes **1-6** in solid state.

No ligand-based emission is noted in the region 400-550 nm, indicating an efficient ligand-to-metal energy transfer process. The five narrow emission peaks centered at 579, 592, 612, 652, and 701 nm, are assigned to $^5D_0 \rightarrow {}^7F_0$, $^5D_0 \rightarrow {}^7F_1$, $^5D_0 \rightarrow {}^7F_2$, $^5D_0 \rightarrow {}^7F_3$ and $^5D_0 \rightarrow {}^7F_4$ transitions, respectively. Among the peaks, the intense $^5D_0 \rightarrow {}^7F_2$ peak points to a highly polarizable chemical environment around the Eu^{3+} ion and is responsible for the red emission.[5,8,21] Moreover, the presence of single and sharp peak in the region of the $^5D_0 \rightarrow {}^7F_0$ at 579 nm, indicates the existence of single chemical environment around the Eu^{3+} ion of point group symmetry C_s, C_n or C_{nv}.[5,8,22] It can be noted from the emission spectra that the luminescence intensity of the ternary complexes (**4**-**6**) significantly enhanced (7-12 fold) as compared to the precursor complexes (**1**-**3**) by the displacement of water molecules from the coordination sphere by the rigid chelating phosphine oxide, DDXPO.

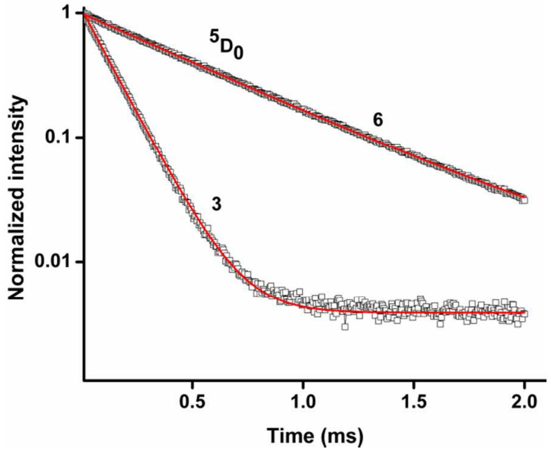

Fig. 6 $^5D_0$ decay profiles for complexes **3** and **6** (solid-state) where emission monitored around 612 nm. The straight lines are the best fits (r^2 = 0.999) considering single-exponential behavior.

Table 2 The radiative (A_{RAD}) and non-radiative (A_{NR}) decay rates, 5D$_0$ lifetime (τ_{obs}), intrinsic quantum Yield (Φ_{Ln}, %), energy transfer efficiency (Φ_{sens}, %), and overall quantum yield ($\Phi_{overall}$, %) for complexes **1**-**6** in the solid state

Compounds		**A_{RAD} (s^{-1})**	**A_{NR} (s^{-1})**	**τ_{obs} (µs)**	**Φ_{Ln} (%)**	**Φ_{sens} (%)**	**$\Phi_{overall}$ (%)**
Eu(APFP)$_3$(H$_2$O)$_2$	(**1**)	1082	2649	275 ± 2	29	41	12 ± 1
Eu(DMAPFP)$_3$(H$_2$O)$_2$	(**2**)	963	8667	105 ± 3	10	13	1 ± 0.1
Eu(DPAPFP)$_3$(H$_2$O)$_2$	(**3**)	1505	6416	129 ± 3	19	17	3 ± 0.3
Eu(APFP)$_3$(DDXPO)	(**4**)	786	481	800 ± 3	63	95	60 ± 6
Eu(DMAPFP)$_3$(DDXPO)	(**5**)	1189	826	498 ± 2	59	42	25 ± 2
Eu(DPAPFP)$_3$(DDXPO)	(**6**)	1152	676	551 ± 1	63	63	40 ± 4

The luminescence decay times (τ_{obs}) for Eu^{3+}-β-diketonate complexes (**1**-**6**) were measured at room temperature using an excitation wavelength that maximizes the Eu^{3+} emission intensity and monitored by the most intense emission line at 612 nm. The lifetime profiles for all the complexes are fitted with single exponentials, thus indicating the presence of only one emissive Eu^{3+} centre. Typical decay profiles for complexes **1**-**6** are displayed in Figs. 6, S8 and S9,† respectively. The corresponding lifetime values are summarized in Table 2. The shorter $^5D_0$ lifetimes noted for Eu^{3+} complexes **1**-**3** may be due to the dominant non-radiative decay channels associated with vibronic coupling on account of the presence of water molecules in the coordination spheres of these complexes.[5,8,23] These values are essentially temperature dependent, with τ_{obs} (at 77 K τ_{obs} = 362, 422 and 339 µs in **1**-**3**, respectively) approximately 2 to 4 fold enhancements in the case of complexes **1**-**3**, while going from 298 to 77 K, thereby reflecting the presence of thermally activated deactivation processes. This effect has been well documented for several other hydrated Eu^{3+}-β-diketonate complexes.[8,24] On the other hand, the lifetime values of complexes **4**-**6** have been significantly enhanced (3-5 times) as compared to their corresponding binary complexes. This may be due to the dramatic decrease of non-radiative decay rates as compared to their precursor complexes. However, the lifetime values of the ternary complexes (**4**-**6**) are almost independent of temperature (τ_{obs} = 551 µs at 298 K; 578 µs in 77 K).

In order to quantify the ability of the ligands designed to sensitize the luminescence of Eu^{3+}, and to draw conclusions about the relationship between the structure and the photophysical properties, it was appropriate to analyze the emission in terms of eqn 1, where $\Phi_{overall}$ and Φ_{Ln} represent the ligand-sensitized and intrinsic luminescence quantum yields of Eu^{3+}; Φ_{sens} represents the efficiency of the ligand-to-metal energy transfer and τ_{obs}/τ_{rad} are the observed and the radiative lifetimes of Eu^{3+} ($^5D_0$):[4b-e,2]

$$\Phi_{overall} = \Phi_{sens} \times \Phi_{Ln} = \Phi_{sens} \times (\tau_{obs}/\tau_{rad}) \quad (1)$$

The intrinsic quantum yields of Eu^{3+} could not be determined experimentally up on direct f-f excitation because of very low absorption intensity.[4c,e,21] Therefore, the radiative lifetimes of Eu^{3+} ($^5D_0$) have been calculated from eqn 2, where n represents the refractive index (1.5) of the medium. $A_{MD,0}$ is the spontaneous emission probability for the $^5D_0/^7F_1$ transition in vacuo (14.65 s^{-1}), and I_{tot}/I_{MD} signifies the ratio of the total integrated intensity of the corrected Eu^{3+} emission spectrum to the integrated intensity of the magnetic dipole $^5D_0/^7F_1$ transition:[25]

$$1/\tau_{rad} = A_{MD,0} \times n^3 \times (I_{tot}/I_{MD}) \quad (2)$$

The intrinsic quantum yield for the designed Eu^{3+}-β-diketonate complexes (**1**-**6**) have been estimated from the ratio τ_{obs}/τ_{rad} and the pertinent values are listed in Table 2. The overall quantum yields ($\Phi_{overall}$), radiative (A_{RAD}) and non-radiative (A_{NR}) decay rates and energy transfer efficiencies ($\Phi_{overall}$) are also presented in Table 2. The substitution of water molecules in [Eu(DPAPFP)$_3$(H$_2$O)$_2$] **3** by the chelating ligand (DDXPO) leads to 4-fold enhancement in the $^5D_0$ lifetime (129 to 551 µs) and 13-fold enhancement in the solid state quantum yield (3 to 40 %). Similarly, in the case of 1-(4 (dimethylamino)phenyl)-4,4,5,5,5-pentafluoro-3-hydroxypent-2-en-1-one based Eu^{3+} complexes, the displacement of water molecules with DDXPO in [Eu(DMAPFP)$_3$(H$_2$O)$_2$] **2** significantly enhances the $^5D_0$ lifetime (105 to 498 µs) and overall quantum yields (1 to 25 %). On the other hand, a 3-fold enhancement in the $^5D_0$ lifetime (275 to 800 µs) and 5-fold enhancement in the overall quantum yield (12 to 60 %) has been noted in Eu^{3+} complex (**4**) containing 1-(4-aminophenyl)-4,4,5,5,5-pentafluoro-3-hydroxypent-2-en-1-one β-diketonate in the presence of DDXPO.

Energy transfer between ligands and Eu^{3+}

To demonstrate the energy transfer process of the derived Eu^{3+} complexes, the energy levels of relevant electronic states of the newly synthesized ligands have been calculated. The singlet (S$_1$) energy levels of the designed β-diketonate and the chelating phosphine oxide ligands were estimated by referring to the upper wavelengths of the UV-vis absorption edges of the corresponding Gd^{3+} complexes (Fig. 7).

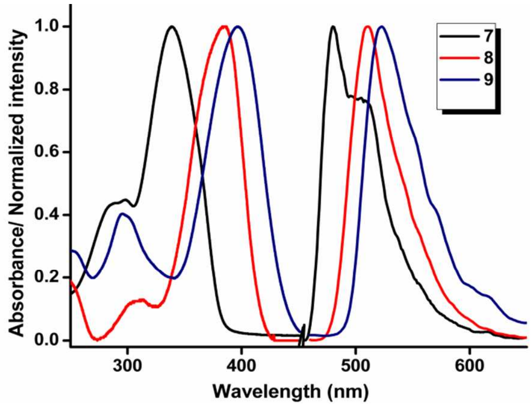

Fig. 7 UV-vis absorption spectra at 298 K (left), and 77 K phosphorescence spectra (right) of the complexes **7**-**9** in THF ($c = 5 \times 10^{-6}$ M).

The pertinent S_1 levels of HAPFP, HDMAPFP, HDPAPFP and DDXPO are found to be 25000 (400 nm), 23981 (416 nm), 23148 (432 nm) and 31850 cm^{-1} (313 nm), respectively. The triplet (T_1) energy levels were calculated from the position of the highest energy band in the corresponding phosphorescence spectra of the Gd^{3+} complexes (Fig. 7).[26] Accordingly, the T_1 of the ligands HAPFP, HDMAPFP, HDPAPFP and DDXPO were found to be 21505 (465 nm), 20833 (480 nm), 20202 (495 nm) and 23470 cm^{-1} (426 nm), respectively. All these values are entirely consistent with the above discussions that the replacement of hydrogen atoms with the electron donating methyl or π-conjugated phenyl groups in aminophenyl based β-diketonate ligands have profound effects on the singlet and triplet states of these ligands. The energy gaps between the Eu^{3+} core ($^5D_0 \sim 17250$ cm^{-1}) and the donor ligand's T_1 levels turns out to be 4255, 3583, 2952 and 6220 cm^{-1} for HAPFP, HDMAPFP, HDPAPFP and DDXPO, respectively. The triplet energy levels of the ligands appears at appreciably higher energy than that of the $^5D_0$ state of Eu^{3+}, thus indicating that the newly developed β-diketonate ligands can act as an efficient sensitizers for the Eu^{3+} ion.[26] On the other hand, the $^5D_1$ state Eu^{3+} (18800 cm^{-1}) is found to be closer to the T_1 of HDPAPFP (ΔE (T_1-$^5D_1$) = 1402 cm^{-1}), which can lead to thermally assisted back energy transfer.[27] However, the T_1 level of HDMAPFP and HAPFP are situated slightly above the $^5D_1$ state of Eu^{3+}. The $^5D_2$ of Eu^{3+} emitting state (21200 cm^{-1}) is higher than the T_1 states of the β-diketonate ligands, which can lead to the thermally assisted back-energy transfer from the central core.[27] It is also noticed that the energy gap between the S_1 and T_1 levels are 3495, 3148, 2946 and 8380 cm^{-1} for HAPFP, HDMAPFP, HDPAPFP and DDXPO, respectively. Also in diphenylamino substituted ligand, the singlet-triplet energy gap is lowered compared to the other ligands as explained before. According to Reinhoudt's empirical rule,[6] the intersystem crossing process becomes effective when ΔE (S_1-T_1) is around 5000 cm^{-1} and hence the intersystem crossing processes are efficient for these ligands. Based on the above observations the photoluminescence mechanism for the derived Eu^{3+} complexes is proposed to involve a ligand sensitized luminescence process (antenna effect).[5,8,28] The typical energy level diagram for complex **6** and the plausible energy transfer pathways are shown in Fig. 8.

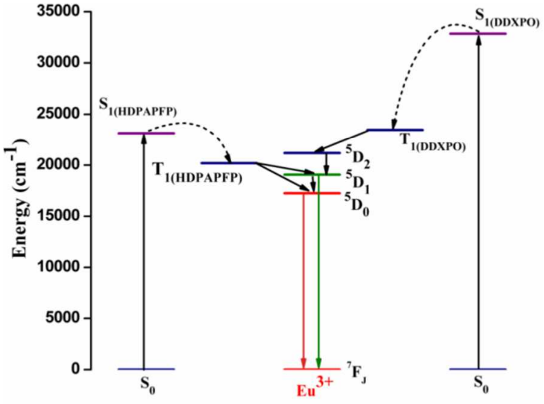

Fig. 8 Schematic energy level diagram and energy transfer processes for the complex **6**. S_1 represents the first excited singlet state and T_1 represents the first excited triplet state.

The photostability of the $Eu(DPAPFP)_3DDXPO$ complex

The photostability of the visible light sensitized Eu^{3+} complex **6** was investigated by means of measuring the luminescence intensity at 612 nm excited at 400 nm at definite time intervals (10 min) for 3 h and the results are shown in Fig. S10.† The results demonstrated that the luminescence intensity of the complex is almost the same even after 3 h of irradiation. This indicates the photostability of the Eu^{3+} complex.

Synthesis, characterization and luminescence studies of hybrid materials EuC-Gel and EuC-PMMA-Gel

The photographs of the designed hybrid gel materials are displayed in Fig. 9. The FT-IR spectra of the $Eu(DPAPFP)_3(DDXPO)$ doped hybrid materials EuC-Gel and EuC-

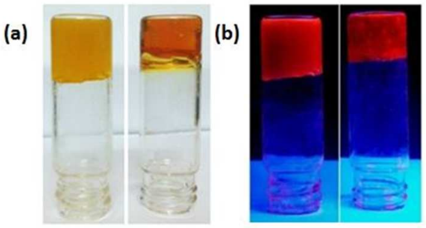

Fig. 9 Photographs of the EuC-PMMA-Gel (left) and EuC-Gel (right) before (a) and after (b) UV irradiation.

PMMA-Gel are shown in Fig. S11.† The formation of Si-O-Si framework in the hybrid materials were confirmed by the peaks observed around 1077 cm^{-1} (ν_{as}, Si-O-Si), 787 cm^{-1} (ν_s, Si-O-Si) and 454 cm^{-1} (δ, Si-O-Si) and in both the hybrid materials which are characteristic of the trialkoxysilyl function.[13d,f,29] The absorption band noted at 1622 cm^{-1} for the both the gels can be assigned to the vibration C=O group of the ligand. A new band at 1736 cm^{-1} noted in the IR spectra of EuC-PMMA-Gel, ascribed to the C=O vibrations of PMMA. The above results suggest the incorporation of the polymer into hybrid material, which may bring small changes *via* coordinating with the central Eu^{3+} ions.

The XRD patterns from 10 to 70° of the hybrid materials are shown in Fig. S12,† exhibiting that the developed hybrid materials are amorphous. The broad peaks noted in both the hybrid materials centered at 22.98° and 23.04°, can be attributed to the siliceous backbone of the hybrids.[13a,29e,30] Further, the absence of any crystalline regions in these hybrid materials correlates the presence of host inorganic networks. The above results clearly indicate that the hybrid materials still hold disordered sequences even after the doping into PMMA matrix, although the polymeric carbon chains of the polymers are essentially regularly ordered. Homogeneous, spherical and interconnected silica particles (~ 500 nm) can be evidenced from SEM investigations of EuC-Gel particles (Fig. 10). On the other hand, the pronounced interconnected sphere like structures in EuC-PMMA-Gel is hard to visualize, in the presence of PMMA.[31]

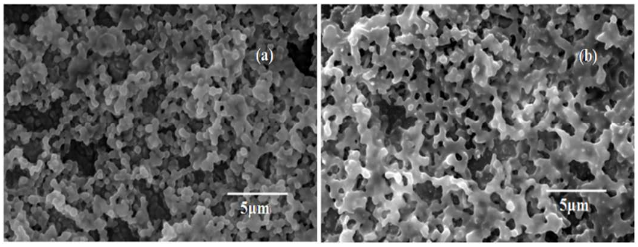

Fig. 10 SEM images of the hybrid materials (a) EuC-Gel and (b) EuC-PMMA-Gel.

The thermal stabilities of EuC-Gel and EuC-PMMA-Gel developed hybrid materials were studied by TG and DTA measurements and the results are given in Fig. S13.† The DTA curve show the thermal stability of the Eu^{3+} ternary complex [353 °C for Eu(DPAPFP)$_3$(DDXPO) decomposition] has been enhanced after incorporating into the hybrid material [414 °C in EuC-Gel decomposition]. It can be noted from the TG curve of EuC-PMMA-Gel that PMMA began to decompose at 398 °C. Further, when the temperature reached 445 °C, the polymer PMMA had departed from the hybrid material.[29e] The results revealed that thermal stability of the hybrid material has enhanced after loading into the hybrid material.

The solid-state absorption spectra of the complex (Eu(DPAPFP)$_3$DDXPO) and the hybrid materials are displayed in Fig. S14†. Compared to the Eu^{3+} ternary complex, a red-shift of the major electronic transition (from 439 to 447 nm) occurs in hybrid materials, which indicates that the electronic distributions of the system have changed when the complexes are embedded in the matrixes and the perturbation is induced by the silanol groups in the hybrid materials.

The excitation and emission spectra of the isolated hybrid materials as solids at room temperature are illustrated in Fig. 11. The excitation spectra of the hybrid materials, which were obtained by monitoring at 612 nm, exhibit a broad excitation band between 300 and 515 nm. This band can be assigned to π-π* electronic transition of the ligands. In the emission spectra of the hybrid materials, only characteristic emissions of Eu^{3+} ions are noted, which indicates that the energy transfer from the ligands to the central Eu^{3+} ions is efficient. The hybrid materials showed characteristic narrow band emissions of Eu^{3+} corresponding to the $^5D_0 \rightarrow {}^7F_J$ (J = 0-4) transitions.

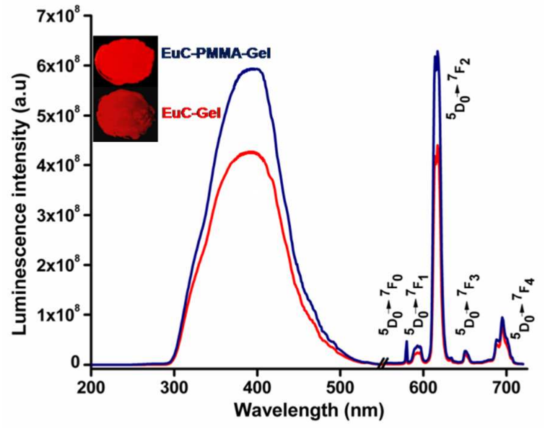

Fig. 11 Room temperature excitation and emission spectra of hybrid materials, EuC-Gel and EuC-PMMA-Gel (Inset photographs show the gels coated on a glass plate).

The five expected peaks of the luminescent spectra are well resolved. The content of the Eu^{3+} complex in hybrid materials and its relative luminescence intensities are listed in Table 3. It is interesting to note that the complex of a unit mass in the silica/polymer matrix is found to be superior to that of corresponding pure complex. The shortening of lifetimes (τ_{obs} = 305 μs in EuC-Gel and 361 μs EuC-PMMA-Gel) in the hybrid materials has been noticed as compared to precursor Eu^{3+} complex (τ_{obs} = 551 μs) (Fig. 12). This might be due to the quenching of abundant O-H oscillators on the silica matrix surface to absorbed complex, which can be clearly seen from the high values of nonradiative decay rates of the hybrid materials (A_{NR}).[29,32] The overall quantum efficiencies of these hybrid materials have been significantly decreased due to the presence of high frequency oscillators in the hybrid materials.

In addition, in the present work, EuC-PMMA-Gel hybrid material has been used as a phosphor to fabricate LED after coating onto a 400 nm emitting InGaN chip and investigated photoluminescence properties (Fig. 13). The LED fabricated with a 400 nm emitting chip exhibited strong red-emission. Thus, the results indicate that EuC-PMMA-Gel hybrid material is an interesting red-emitting material excited by blue-light, making it a potential candidate in many photonic applications without using UV radiation for excitation.[7b]

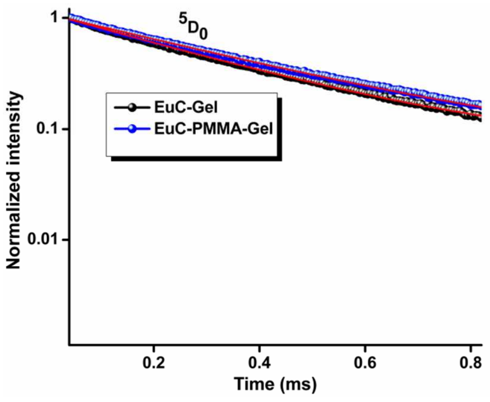

Fig. 12 $^5D_0$ decay profiles for EuC-Gel and EuC-PMMA-Gel (solid-state) where emission monitored around 612 nm. The straight lines are the best fits (r^2 = 0.999) considering single-exponential behavior.

Table 3 Luminescence intensities, content of the Eu^{3+} complex, radiative-nonradiative decay rates and the photoluminescence quantum yields of $Eu(DPAPFP)_3DDXPO$, EuC-PMMA-Gel and EuC-Gel samples

Compounds	**$Eu(DPAPFP)_3DDXPO$**	**EuC-Gel**	**EuC-PMMA-Gel**
Content of the complex **6** (wt %)	100	23.8	18.5
Relative intensity of $^5D_0 \rightarrow {}^7F_2$	8.02×10^8	4.37×10^8	6.31×10^8
Unit mass luminescence intensity	8.02×10^8	1.84×10^9	3.41×10^9
A_{RAD} (s^{-1})	1152	1031	953
A_{NR} (s^{-1})	676	2294	1849
τ_{obs} (μs)	551 ± 1	305 ± 2	361 ± 2
Φ_{Ln} (%)	63	31	34
Φ_{sens} (%)	63	56	63
$\Phi_{overall}$ (%)	40 ± 4	18 ± 2	22 ± 2

Conclusions

In conclusion, a series of new antenna complexes of Eu^{3+} based on aminophenyl based polyfluorinated β-diketonate ligands in the absence and presence of a chelating phosphine oxide has been developed. Most importantly, among the designed complexes, Eu^{3+}-triphenylamine β-diketonate ternary complex exhibits intense red-emission under blue light excitation (λ_{ex} = 400 nm) with an impressive quantum yield ($\Phi_{overall}$ = 40 %) and $^5D_0$ lifetime values (τ_{obs} = 551 μs). Suitably expanded π-conjugation in the complex molecules successfully red-shifted the excitation band of the Eu^{3+}-β-diketonate complexes to the visible region. Contrary to the above, the electron-donating dimethylamino group (Hammett constant: σ_p = -0.83) containing Eu^{3+}-β-diketonate complexes moderately shifted the excitation maximum in the UV region from 370 to 380 nm as compared to unsubstituted aminophenyl (Hammett constant: σ_p = -0.66) Eu^{3+} complexes. In order to improve the thermal and mechanical stability, the derived highly luminescent Eu^{3+} complex has been embedded into a hybrid silica/polymer material by sol-gel method. The resultant hybrid material EuC-PMMA-Gel displays efficient unit mass luminescence emission (3.41×10^9) and greater thermal stability (398 °C) as compared to precursor ternary Eu^{3+} complex [unit mass luminescence emission = 8.02×10^8 ; thermal stability = 353 °C]. In addition, the InGaN LED developed by coating the EuC-PMMA-Gel hybrid material displays bright red-emission under blue light excitation. The present results clearly demonstrate that Eu^{3+}-triphenylamine based β-diketonate complexes may find potential applications in many optoelectronic technologies.

Acknowledgements

One of the authors T. V. Usha Gangan also acknowledges UGC, New Delhi for the award of Senior Research Fellowship and AcSIR for Ph.D registration.

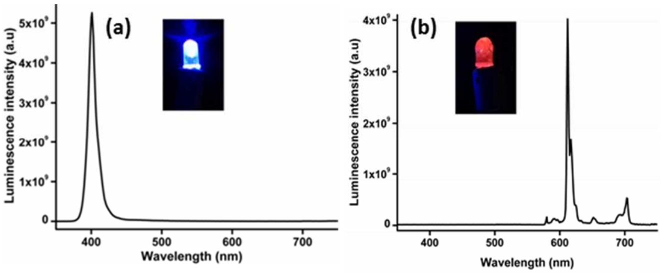

Fig. 13 Emission spectra of the blue LED (left) and EuC-PMMA-Gel coated blue LED (right). Inset: photographs of the LEDs in working state.

Notes and references

1 (*a*) J.-C. G. Bünzli, *Chem. Rev.*, 2010, **110**, 2729; (*b*) M. C. Heffern, L. M. Matosziuk and T. J. Meade, *Chem. Rev.,* 2014, **114**, 4496; (*c*) X. Wang, H. Chang, J. Xie, B. Zhao, B. Liu, S. Xu, W. Pei, N. Ren, L. Huang and W. Huang, *Coord. Chem. Rev.*, 2014, **273**, 201; (*d*) J.-C. G. Bünzli and S. V. Eliseeva, *Chem. Sci.*, 2013, **4**, 1939.

2 (*a*) J. Feng and H. Zhang, *Chem. Soc. Rev.,* 2013, **42**, 387; (*b*) A. de Bettencourt-Dias, *Dalton Trans.*, 2007, **22**, 2229; (*c*) L. D. Carlos, R. A. S. Ferreira, V. de Zea Bermudez, B. J.-Lopezc and P. Escribano, *Chem. Soc. Rev.,* 2011, **40**, 536.

3 (*a*) S. V. Eliseeva and J.-C. G. Bünzli, *Chem. Soc. Rev.*, 2010, **39**, 189; (*b*) S. V. Eliseeva and J.-C. G. Bünzli, *New J. Chem.*, 2011, **35**, 1165; (*c*) L. D. Carlos, R. A. S. Ferreira, V. Z. Bermudez and S. J. L. Ribeiro, *Adv. Mater.*, 2009, **21**, 509.

4 (*a*) C. P. Montgomery, B. S. Murray, E. J. New, R. Pal and D. Parker, *Acc. Chem. Res.*, 2009, **42**, 925; (b) L. Armelao, S. Quici, F. Barigelletti, G. Accorsi, G. Bottaro, M. Cavazzini and E. Tondello, *Coord. Chem. Rev.*, 2010, **254**, 487; (*c*) Y. Ma and Y. Wang, *Coord. Chem. Rev.*, 2010, **254**, 972; (*d*) K. Binnemans, *Chem. Rev.*, 2009, **109**, 4283; (*e*) J.-C. G. Bünzli and C. Piguet, *Chem. Soc. Rev.*, 2005, **34**, 1048; (*f*) P. P. Lima, M. M. Nolasco, F. A. A. Paz, R. A. S. Ferreira, R. L. Longo, O. L. Malta and L. D. Carlos, *Chem. Mater.*, 2013, **25**, 586.

5 (*a*) D. B. A. Raj, S. Biju and M. L. P. Reddy, *Inorg. Chem.*, 2008, **47**, 8091; (*b*) S. Biju, D. B. A. Raj, M. L. P. Reddy and B. M. Kariuki, *Inorg. Chem.*, 2006, **45**, 10651; (*c*) S. Biju, M. L. P. Reddy, A. H. Cowley and K. V. Vasudevan, *Cryst. Growth Des.*, 2009, **9**, 3562; (*d*) S. Biju, N. Gopakumar, J.-C. G. Bünzli, R. Scopelliti, H. K. Kim and M. L. P. Reddy, *Inorg. Chem.*, 2013, **52**, 8750; (*e*) D. B. A. Raj, B. Francis, M. L. P. Reddy, R. R. Butorac, V. M. Lynch and A. H. Cowley, *Inorg. Chem.*, 2010, **49**, 9055; (*f*) D. B. A. Raj, S. Biju and M. L. P. Reddy, *Dalton Trans.*, 2009, **36**, 7519; (*g*) B. Francis, D. B. A. Raj and M. L. P. Reddy, *Dalton Trans.*, 2010, **39**, 8084; (*h*) J. A. Fernandes, R. A. Sá Ferreira, M. Pillinger, L. D. Carlos, I. S. Goncalves, and P. J. A. R.-Claro, *Eur. J. Inorg. Chem.,* 2004, **19**, 3913; (*i*) L. F. Smith, B. A. Blight, H.-J. Park and S. Wang, *Inorg. Chem.*, 2014, **53**, 8036; (*j*) J. Leng, H. Li, P. Chen, W. Sun, T. Gao and P. Yan, Dalton Trans., 2014, **43**, 12228; (*k*) G. Shao, H. Yu, N. Zhang, Y. He, K. Feng, X. Yang, R. Cao and M. Gong, *Phys. Chem. Chem. Phys.*, 2014, **16**, 695; (*l*) X. Chen, P. Zhang, T. Wang, and H. Li, *Chem. Eur. J.*, 2014, **20**, 2551.

6 F. J. Steemers, W. Verboom, D. N. Reinhoudt, E. B. Vander Tol and J. W. Verhoeven, *J. Am. Chem. Soc.*, 1995, **117**, 9408.

7 (*a*) P. He, H. H. Wang, S. G. Liu, J. X. Shi, G. Wang and M. L. Gong, *Inorg. Chem.*, 2009, **48**, 11382; (*b*) P. He, H. H. Wang, H. G. Yan, W. Hu, J. X. Shi and M. L. Gong, *Dalton Trans.*, 2010, **39**, 8919; (*c*) J. Wu, Z. Ye, G. Wang, D. Jin, J. Yuan, Y. Guan and J. Piper, *J. Mater. Chem.*, 2009, **19**, 1258; (*d*) J. Wu, G. Wang, D. Jin, J. Yuan, Y. Guan and J. Piper, *Chem. Commun.*, 2008, 365; (*e*) M. Shi, C. Ding, J. Dong, H. Wang, Y. Tian and Z. Hu, Phys. *Chem. Chem. Phys.*, 2009, **11**, 5119; (*f*) M. H. V. Werts, M. A. Duin, J. W. Hofstraat and J. W. Verhoeven, *Chem. Commun.*, 1999, **9**, 799.

8 (*a*) M. L. P. Reddy, V. Divya and R. Pavithran, *Dalton Trans.*, 2013, **42**, 15249; (*b*) V. Divya, R. O. Freire and M. L. P. Reddy, *Dalton Trans.*, 2011, **40**, 3257; (*c*) V. Divya, S. Biju, R. Luxmi Varma and M. L. P. Reddy, *J. Mater. Chem.*, 2010, **20**, 5220; (*d*) V. Divya and M. L. P. Reddy, *J. Mater. Chem. C.*, 2013, **1**, 160; (*e*) V. Divya, V. Sankar, K. G. Raghu and M. L. P. Reddy, *Dalton Trans.*, 2013, **42**, 12317.

9 (*a*) R. V. Deun, P. Fias, P. Nockemann, K. V. Hecke, L. V. Meervelt, and K. Binnemans, *Inorg. Chem.*, 2006, **45**, 10416; (*b*) C. Yang, L.-M. Fu, Y. Wang, J.-P. Zhang, W.-T. Wong, X.-C. Ai, Y.-F. Qiao, B.-S. Zou, and L.-L. Gui, *Angew. Chem. Int. Ed.*, 2004, **43**, 5010; (*c*) F. Xue, Y. Ma, L. Fu, R. Hao, G. Shao, M. Tang, J. Zhang and Y. Wang, *Phys. Chem. Chem. Phys.*, 2010, **12**, 3195; (*d*) M. Shi, C. Ding, J. Dong, H. Wang,Y. Tian and Z. Hu, *Phys. Chem. Chem. Phys.*, 2009, **11**, 5119; (*e*) G. Zucchi,V. Murugesan, D. Tondelier, D. Aldakov, T. Jeon, F. Yang, P. Thuéry, M. Ephritikhine and B. Geffroy, *Inorg. Chem.*, 2011, **50**, 4851.

10 (*a*) K. Sakanoue, M. Motoda, M. Sugimoto and S. Sakaki, *J. Phys. Chem. A.*, 1999, **103**, 5551; (*b*) J.-S. Yang, S.-Y. Chiou, and K.-L. Liau, *J. Am. Chem. Soc.*, 2002, **124**, 2518.

11 (*a*) L.-N. Sun, J.-Bo Yu, G.-L. Zheng, H.-J. Zhang, Q.-G. Meng, C.-Y. Peng, L.-S. Fu, F.-Y. Liu and Y.-N. Yu, *Eur. J. Inorg. Chem.*, 2006, 3962; (*b*) A.-S. Chauvin, F. Gumy, I. Matsubayashi, Y. Hasegawa, and J.-C. G. Bünzli, *Eur. J. Inorg. Chem.*, 2006, 473; (*c*) Y. Hasegawa, Y. Wada, S. Yanagid, J. *Photochem. Photobiol. C.*, 2004, **5**, 183; (*d*) Y. Hasegawa, T. Ohkubo, K. Sogabe, Y. Kawamura, Y. Wada, N. Nakashima and S. Yanagida, *Angew. Chem., Int. Ed.*, 2000, **39**, 357.

12 (a) S. Biju, M. L. P. Reddy, A. H. Cowley and K. V. Vasudevan, *J. Mater. Chem.*, 2009, **19**, 5179; (*b*) S. Sivakumar and M. L. P. Reddy, *J. Mater. Chem.*, 2012, **22**, 10852; (*c*) S. Biju, R. O. Freire, Y. Kyung Eom, R. Scopelliti, J.-C. G. Bünzli and H. K. Kim, *Inorg. Chem.*, 2014, **53**, 8407; (*d*) R. Shunmugam and G. N. Tew, *J. Am. Chem. Soc.*, 2005, **127**, 13567; (*e*) B. Chen and J. Feng, *J. Phys. Chem. C.,* 2015, **119**, 7865; (*f*) W. Fan, J. Feng, S. Song, Y. Lei, L. Zhou, G. Zheng, S. Dang, S. Wang and H. Zhang, *Nanoscale.*, 2010, **2**, 2096; (*g*) J. Kai, D. F. Parrab and H. F. Brito, *J. Mater. Chem.*, 2008, **18**, 4549; (*h*) O. Moudam, B. C. Rowan, M. Alamiry, P. Richardson, B. S. Richards, A. C. Jones and N. Robertson, *Chem. Commun.*, 2009, 6649.

13 (*a*) D. Haranath, S. Mishra, A. G. Joshi, S. Sahai and V. Shanker, *Nano-Micro Lett.*, 2011, **3**, 141; (*b*) P. P. Lima, R. A. S. Ferreira, R. O. Freire, F. A. Almeida Paz, L. Fu, S. Alves Jr, L. D. Carlos and O. L. Malta, *ChemPhysChem.*, 2006, **7**, 735; (*c*) J. D. Mackenzie and E. P. Bescher, *Acc. Chem. Res.*, 2007, **40**, 810; (*d*) X. Guo, H. Guo, L. Fu, H. Zhang, L. D. Carlos, R. Deng and J. Yu, *J. Photochem. Photobiol. A.*, 2008, **200**, 318; (*e*) L. D. Carlos, R. A. Sá Ferreira, J. P. Rainho, V. de Zea Bermudez, *Adv. Funct. Mater.*, 2002, **12**, 819; (*f*) L. N. Sun, H. J. Zhang, Q. G. Meng, F. Y. Liu, L. N. Fu, C. Y. Peng, J. B. Yu, G. L. Zheng and S. B. Wang, *J. Phys. Chem. B.*, 2005, **109**, 6174.

14 (*a*) D. B. A. Raj, S. Biju and M. L. P. Reddy, *J. Mater. Chem.*, 2009, **19**, 7976; (*b*) P. Escribano, B. J.-Lopéz, J. P.-Aragó, E. Cordoncillo, B. Viana and C. Sanchez, *J. Mater. Chem.*, 2008, **18**, 23; (*c*) B. Yan and Y.-J. Li, *J. Mater. Chem.*, 2011, **21**, 18454; (*d*) L. Sun, W. Mai, S. Dang, Y. Qiu,W. Deng, L. Shi,W. Yanaand H. Zhang, *J. Mater. Chem.*, 2012, **22**, 5121; (*e*) P. Lenaerts, A. Storms, J. Mullens, J. D'Haen, C. G.-Walrand, K. Binnemans, and K. Driesen, *Chem. Mater.*, 2005, **17**, 5194; (*f*) E. DeOliveira, C. R. Neri, O. A. Serra, and A. G. S. Prado,

Chem. Mater., 2007, **19**, 5437; (*g*) D. Zhang, X. Wang, Z.-an Qiao, D. Tang, Y. Liu, and Q. Huo, *J. Phys. Chem. C*., 2010, **114**, 12505.

15 (*a*) L. Maggini, H. Traboulsi, K. Yoosaf, J. Mohanraj, J. Wouters, O. Pietraszkiewicz, M. Pietraszkiewicz, N. Armaroliand D. Bonifazi, *Chem. Commun*., 2011, **47**, 1625; (*b*) L. Maggini, J. Mohanraj, H. Traboulsi, A. Parisini, G. Accorsi, N. Armaroli and D. Bonifazi, *Chem. Eur. J*., 2011, **17**, 8533; (*c*) X. Xin, M. Pietraszkiewicz, O. Pietraszkiewicz, O. Chernyayeva, T. Kalwarczyk, E. Gorecka, D. Pociecha, H. Li and R. Hołyst, *Carbon.*, 2012, **50**, 436; (*d*) B. Sitharaman, S. Rajamani and Pramod, K. Avti, *Chem. Commun*., 2011, **47**, 1607; (*e*) C. Zhao, Y. Song, K. Qu, J. Ren, and X. Qu, *Chem. Mater*., 2010, **22**, 5718; (*f*) J. Mohanraj and N. Armaroli, *J. Phys. Chem. Lett*., 2013, **4**, 767; (*g*) L. Maggini, F. M. Toma, L. Feruglio, J. M. Malicka, T. D. Ros, N. Armaroli, M. Prato and D. Bonifazi, *Chem.–Eur. J*., 2012, **18**, 5889.

16 (*a*) J. C. De Mello, H. F. Wittmann and R. H. Friend, *Adv. Mater*., 1997, **9**, 230; (*b*) L.-O. Pålsson and A. P. Monkman, *Adv. Mater*., 2002, **14**, 757; (*c*) B. K. Shah, D. C. Neckers, J. Shi, E. W. Forsythe and D. Morton, *Chem. Mater.*, 2006, **18**, 603.

17 (*a*) M. Cölle, J. Gmeiner, W. Milius, H. Hillebrecht and W. Brütting, *Adv. Funct. Mater.*, 2003, **13**, 108; (*b*) N. S. Saleesh Kumar, S. Varghese, N. P. Rath and S. Das, *J. Phys. Chem. C*, 2008, **112**, 8429; (*c*) S. V. Eliseeva, O. V. Kotova, F. Gumy, S. N. Semenov, V. G. Kessler, L. S. Lepnev, J.-C. G. Bünzli and N. P. Kuzmina, *J. Phys. Chem. A.*, 2008, **112**, 3614.

18 (*a*) N. M. Shavaleev, R. Scopelliti, F. Gumy and J.-C. G. Bünzli, *Eur. J. Inorg. Chem.*, 2008, **9**, 1523; (*b*) A. W. Woodward, A. Frazer, A. R. Morales, J. Yu, A. F. Moore, A. D. Campiglia, E. V. Jucov, T. V. Timofeevab and K. D. Belfield, *Dalton Trans*., 2014, **43**, 16626; (*c*) D. Nie, Z. Chen, Z. Bian, J. Zhou, Z. Liu, F. Chen, Y. Zhao and C. Huang, *New J. Chem*., 2007, **31**, 1639.

19 (*a*) C. M. Whitaker, E. V. Patterson, K. L. Kott and R. J. McMahon, *J. Am. Chem. Soc*., 1996, **118**, 9966; (*b*) G. Park, C. S. Ra and B. R. Cho, *Bull. Korean Chem. Soc*., 2003, **24**, 1671; (*c*) J. E. Haley, D. M. Krein, J. L. Monahan, A. R. Burke, D. G. McLean, J. E. Slagle, A. Fratini and T. M. Cooper, *J. Phys. Chem*., 2011, **115**, 265; (*d*) L.-H. Ma, Z.-B. Chen, Y.-B. Jiang, *Chem. Phys. Lett*., 2003, **372**, 104-113; (*e*) G.-J. Huang and J.-S. Yang, *Chem. Asian J.*, 2010, **5**, 2075; (*f*) J.-S. Yang, K.-L. Liau, C.-M.Wang and C.-Y. Hwang, *J. Am. Chem. Soc*., 2004, **126**, 12325.

20 (*a*) X. Mou, Y. Wu, S. Liu, M. Shi, X. Liu, C. Wang, S. Sun, Q. Zhao, X. Zhoua and W. Huang, *J. Mater. Chem*., 2011, **21**, 13951; (*b*) C. Hansch, A. Leo and R. W. Taft, *Chem. Rev*., **97**, 165; (*c*) T. Karatsu, M. Takahashi, S. Yagai and A. Kitamura, *Inorg. Chem*., 2013, **52**, 12338.

21 (*a*) M. H. V. Werts, R. T. F. Jukes and J. W. Verhoeven, *Phys. Chem. Chem. Phys*., 2002, **4**, 1542; (*b*) Z. Ahmed and K. Iftikhar, *J. Phys. Chem. A.*, 2013, **117**, 11183; (*c*) E. E. S. Teotonio, H. F. Brito, M. C. F. C. Felinto, L. C. Thompson, V. G. Young, O. L. Malta, *J. Mol. Struct.*, 2005, **751**, 85.

22 (*a*) J. Shi, Y. Hou, W. Chu, X. Shi, H. Gu, B. Wang, and Z. Sun, *Inorg. Chem*., 2013, **52**, 5013; (*b*) G. Shao, H. Yu, N. Zhang, Y. He, K. Feng, X. Yang, R. Cao and M. Gong, *Phys. Chem. Chem. Phys.,* 2014, **16**, 695; (*c*) J. Kai, D. F. Parra and H. F. Brito, *J. Mater. Chem*., 2008, **18**, 4549.

23 (*a*) G. F. de Sa, O. L. Malta, C. de Mello Donega, A. M. Simas, R. L. Longo, P. A. Santa-Cruz and E. F. da Silva Jr., *Coord. Chem. Rev*., 2000, **196**, 165; (*b*) B. Makhinson, A. K. Duncan, A. R. Elam, A. de Bettencourt-Dias, C. D. Medley, J. E. Smith, and E. J. Werner, *Inorg. Chem*., 2013, **52**, 6311.

24 (*a*) A. Dossing, *Eur. J. Inorg. Chem*., 2005, 1425; (*b*) A. Beeby, I. M. Clarkson, R. S. Dickins, S. Faulkner, D. Parker, L. Royle, A. S. de Sousa, J. A. G. Williams and M. Woods, *J. Chem. Soc. Perkin Trans*., 1999, **2**, 493.

25 N. M. Shavaleev, S. V. Eliseeva, R. Scopelliti and J.-C. G. Bünzli, *Inorg. Chem*., 2010, **49**, 3927.

26 (*a*) Q.-Y. Yang, M. Pan, S.-C. Wei, C.-W. Hsu, J.-M. Lehn and C.-Y. Su, *CrystEngComm*., 2014, **16**, 6469; (*b*) M. Shi, F. Li, T. Yi, D. Zhang, H. Hu and C. Huang, *Inorg. Chem*., 2005, **44**, 8929; (*c*) S. I. Klink, L. Grave, D. N. Reinhoudt, and F. C. J. M. van Veggel, *J. Phys. Chem. A.,* 2000, **104***,* 5457; (*d*) H. Xin, M. Shi, X. C. Gao, Y. Y. Huang, Z. L. Gong, D. B. Nie, H. Cao, Z. Q. Bian, F. Y. Li, and C. H. Huang, *J. Phys. Chem. B.*, 2004, **108**, 10796.

27 (*a*) N. Armaroli, G. Accorsi, F. Barigelletti, S. M. Couchman, J. S. Fleming, N. C. Harden, J. C. Jeffery, K. L. V. Mann, J. A. McCleverty, L. H. Rees, S. R. Starling and M. D. Ward, *Inorg. Chem.*, 1999, **38**, 5769; (*b*) M. Latva, H. Takalo, V.-M. Mukkala, C. Matachescu, J. C. Rodriguez-Ubis and J. Kankare, *J. Lumin.*, 1997, **75**, 149.

28 (*a*) J.-M. Lehn, *Angew. Chem. Int. Ed.*, 1990, **29**, 1304; (*b*) S. Petoud, S. M. Cohen, J.-C. G. Bünzli and K. N. Raymond, *J. Am. Chem. Soc.*, 2003, **125**, 13324; (*c*) A. R. Ramya, D. Sharma, S. Natarajan and M. L. P. Reddy, *Inorg. Chem*., 2012, **51**, 8818.

29 (*a*) L.-N. Sun, H.-J. Zhang, J.-B. Yu, Q.-G. Meng, F.-Y. Liu and C.-Y. Peng, *J. Photochem. Photobiol. A*., 2008, **193**, 153; (*b*) L. Sun, Y. Qiu, T. Liu, J. Z. Zhang, S. Dang, J. Feng, Z. Wang, H. Zhang and L. Shi, *ACS Appl. Mater. Interfaces.*, 2013, **5**, 9585; (*c*) X. Guo, H. Guo, L. Fu, L. D. Carlos, R. A. S. Ferreira, L. Sun, R. Deng and H. Zhang, *J. Phys. Chem. C.*, 2009, **113**, 12538; (*d*) J. Xu, Y. Ma, L. Jia , X. Huang, Z. Deng, H. Wana, W. Liu and Yu Tang, *Materials Chemistry and Physics*., 2012, **133**, 78; (*e*) X. Huang, Q. Wang, X. Yan, J. Xu, W. Liu, Q. Wang and Y. Tang, *J. Phys. Chem. C*., 2011, **115**, 2332.

30 L. Guo, B. Yan, J.-L. Liu, K. Sheng and X.-L. Wang, *Dalton Trans*., 2011, **40**, 632.

31 P. C. R. Soares-Santos, H. I. S. Nogueira, V. Felíx, M. G. B. Drew, R. A. Sá Ferreira, L. D. Carlos and T. Trindade, *Chem. Mater*., 2003, **15**, 100.

32 J. G.-Torres, P. B.-Jimenez, E. T.-Calleja, M. Kennedy, H. Ahmed, J. Doran, D. G.-Tauste, L. Bautista and M. D. Pirriera, *J. Photochem. Photobiol. A*., 2014, **283**, 8.